Table S1: Mid-point depth and thickness of each model layer

Model level	Depth (m)	Thickness (m)
1	2.9	5.8
2	10.5	9.4
3	24	18
4	49	32
5	89	49
6	152	76
7	253	127
8	426	219
9	718	365
10	1175	550
11	1815	730
12	2613	866
13	3521	949
14	4492	993
15	5496	1016

Table S2: Sources of seawater iodide and iodate observations used for model development and parameter optimisation ('Dev.') and model evaluation ('Ev.').

Region	Source	Method of acquisition	Use	
			Dev.	**Ev.**
Global (iodide)	Chance et al., 2019	Retrieved from public archive	Y	Y
Global (iodate)	Chance et al., 2019	Provided by authors	Y	Y
Atlantic meridional transect (subsurface concentrations)	Truesdale et al., 2000	Digitised from publication	Y	Y
North Atlantic (subsurface concentrations)	Waite et al., 2006	Digitised from publication	Y	Y
Subtropical Atlantic and pacific (subsurface concentrations)	Campos et al., 1996	Digitised from publication	N	Y
English Channel	Jones et al., 2024	Provided by authors	Y	Y
Atlantic meridional transect	Yang et al., 2025	Provided by authors	Y	Y
High Arctic	Brown et al., 2024	Provided by authors	Y	Y
North Pacific meridional transect	Moriyasu et al., 2023	Retrieved from public archive	Y	Y
Eastern tropical north Pacific	Moriyasu et al., 2020	Retrieved from public archive	Y	Y
Eastern tropical north Pacific	Carrano et al., 2020	Digitised from publication	Y	Y
Southern Ocean (Amundsen Sea)	Xing et al., 2020	Digitised from publication	Y	Y
Eastern tropical south Pacific	Rapp et al., 2020	Retrieved from public archive	Y	Y
sub-Arctic Pacific	Qi et al., 2023	Digitised from publication	N	Y
Subtropical Atlantic	Unpublished data	Provided by authors	N	Y
Subtropical north Pacific	Streanga et al., 2024	Digitised from publication	N	Y
Subtropical Atlantic	Schur et al., 2024	Digitised from publication	N	Y
Central Arctic Ocean	Zhang et al., 2023	Digitised from publication	N	Y

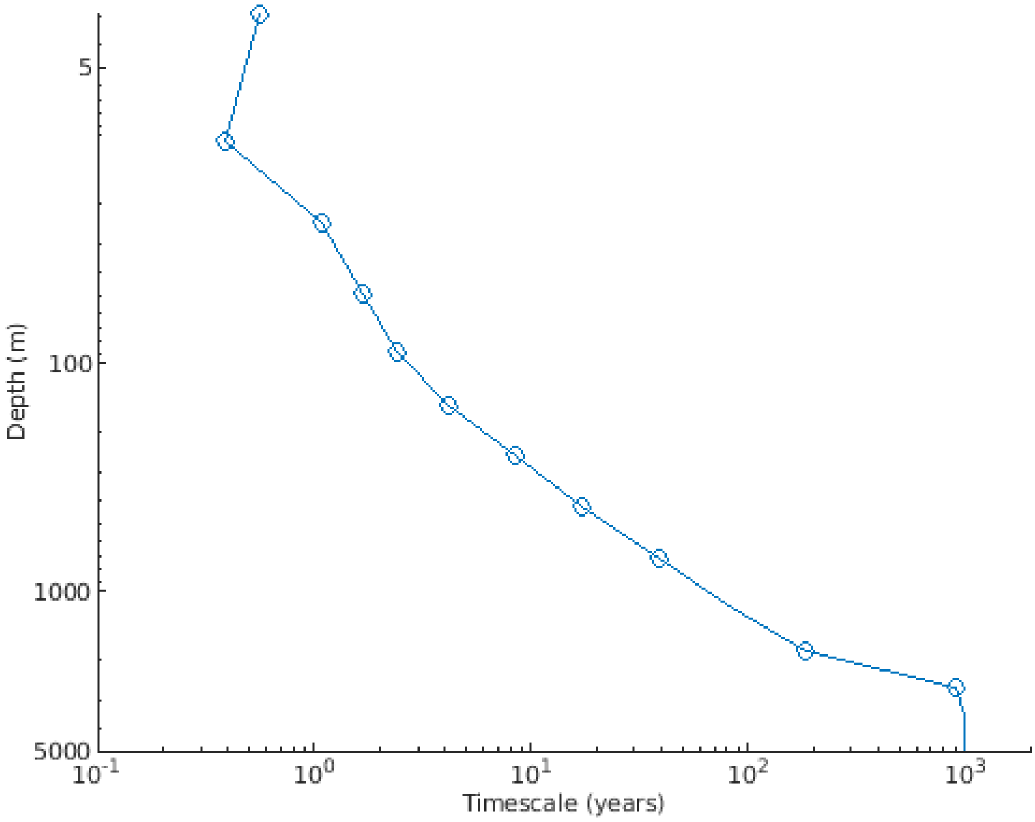

Fig. S1: Vertical profile of ammonium oxidation lifetime derived from the best fit of modelled iodide to observations during model development.

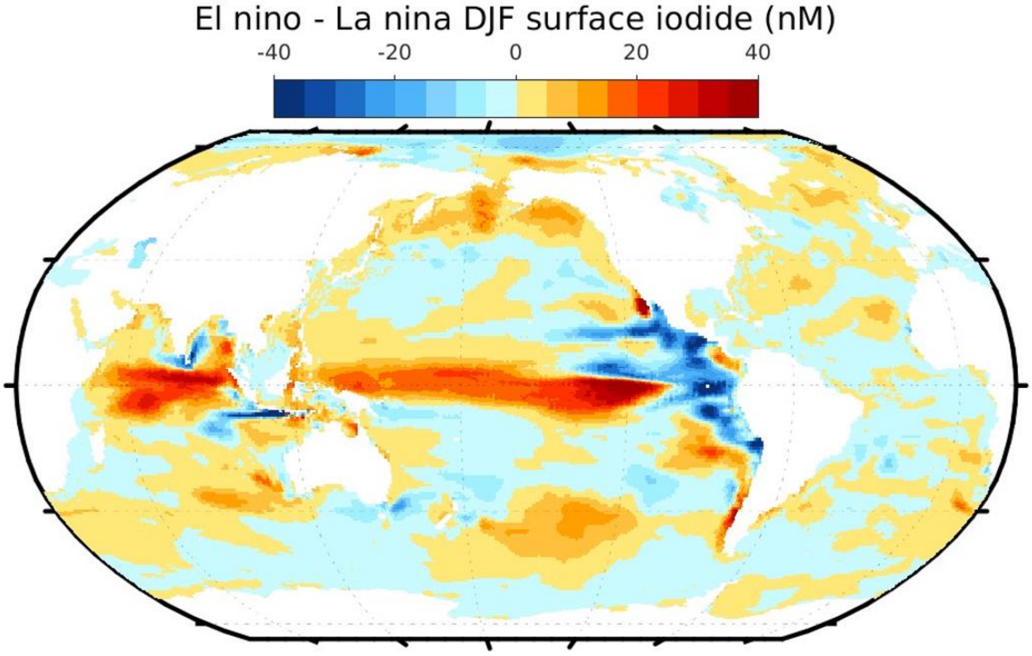

Fig. S2: Difference in average sea surface iodide concentrations predicted by I-CYCLE between El Niño and La Niña years constructed from composites from the control simulation, for the months December to February.

(a)

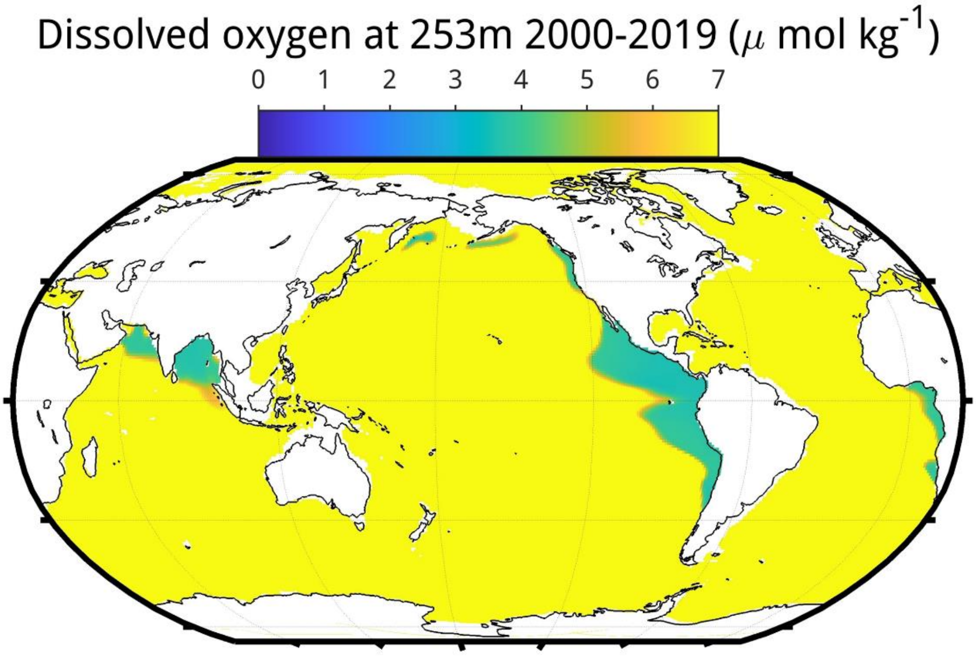

(b)

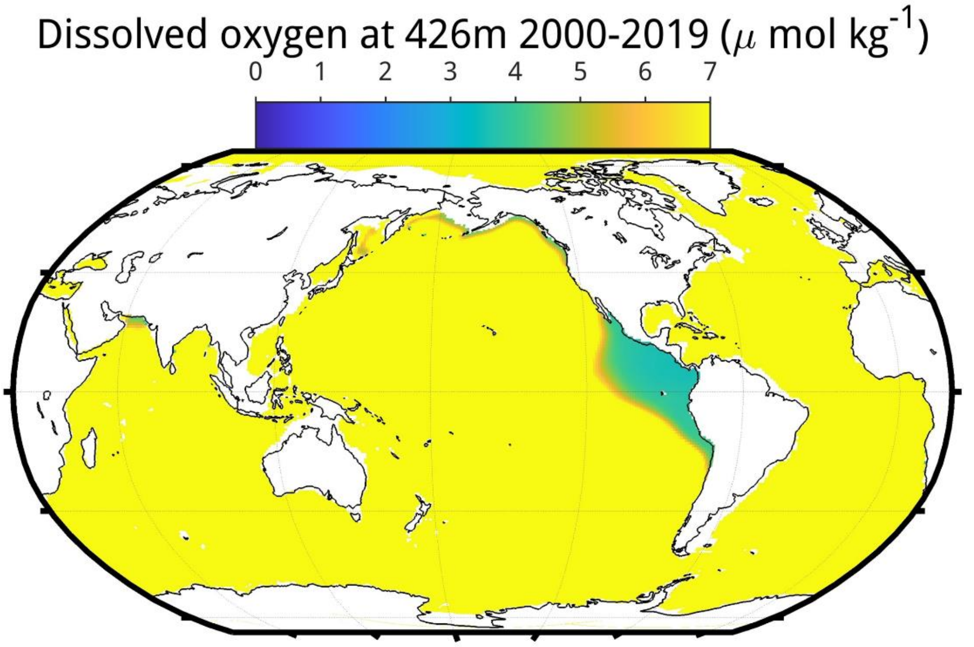

Fig. S3: Present day dissolved oxygen concentration (μmol kg^{-1}) simulated by UKESM 1.0 at (a) 253 m and (b) 426 m depths

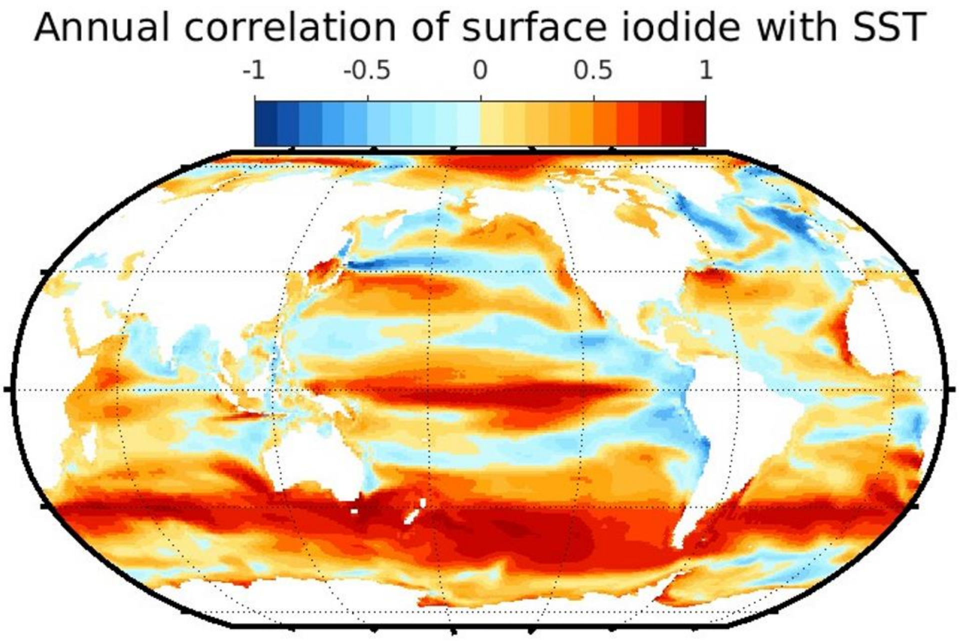

Fig. S4: Correlation of simulated sea surface iodide concentrations with SST over the course of the control simulation for each grid point.

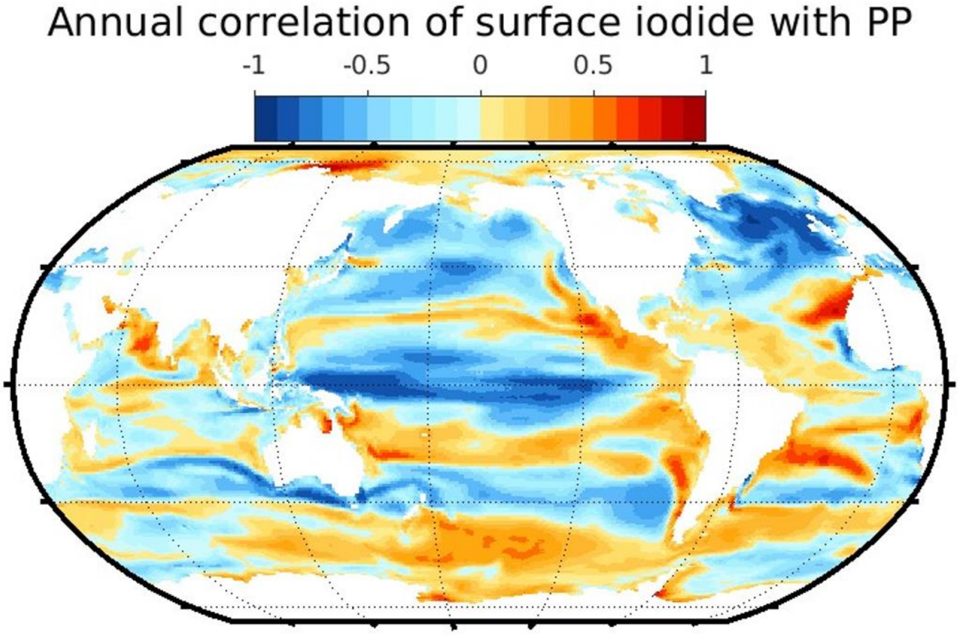

Fig. S5: Correlation of simulated sea surface iodide concentrations with UK-ESM primary productivity over the course of the control simulation for each grid point.

References

Brown, L. V., Pound, R. J., Jones, M. R., Rowlinson, M. J., Chance, R., Jacobi, H.-W., Frey, M. M., Archer, S. D., Arndt, S., Barten, J. G. M., Blomquist, B. W., Dadic, R., Ganzeveld, L. N., Hannula, H.-R., Helmig, D., Jaggi, M., Krampe, D., Macfarlane, A. R., Miller, S., Schneebeli, M., and Carpenter, L. J.: Iodine speciation in snow during the MOSAiC expedition and its implications for Arctic iodine emissions, Faraday Discuss., 258, 441-472, 10.1039/d4fd00178h, 2025.

Campos, M. L. A. M., Farrenkopf, A. M., Jickells, T. D., and Luther, G. W.: A comparison of dissolved iodine cycling at the Bermuda Atlantic Time-series Station and Hawaii Ocean Time-series Station, Deep Sea Research Part II: Topical Studies in Oceanography, 43, 455-466, https://doi.org/10.1016/0967-0645(95)00100-X, 1996.

Carrano, M. W., Yarimizu, K., Gonzales, J. L., Cruz-López, R., Edwards, M. S., Tymon, T. M., Küpper, F. C., and Carrano, C. J.: The influence of marine algae on iodine speciation in the coastal ocean, Algae, 35, 167-176, 10.4490/algae.2020.35.5.25, 2020.

Chance, R. J., Tinel, L., Sherwen, T., Baker, A. R., Bell, T., Brindle, J., Campos, M. L. A. M., Croot, P., Ducklow, H., Peng, H., Hopkins, F., Hoogakker, B., Hughes, C., Jickells, T. D., Loades, D., Macaya, D. A. R., Mahajan, A. S., Malin, G., Phillips, D., Roberts, I., Roy, R., Sarkar, A., Sinha, A. K., Song, X., Winkelbauer, H., Wuttig, K., Yang, M., Peng, Z., and Carpenter, L. J.: Global sea-surface iodide observations, 1967–2018, Scientific Data, 6, 286, 10.1038/s41597-019-0288-y, 2019.

Jones, M. R., Chance, R., Bell, T., Jones, O., Loades, D. C., May, R., Tinel, L., Weddell, K., Widdicombe, C., and Carpenter, L. J.: Iodide, iodate & dissolved organic iodine in the temperate coastal ocean, Frontiers in Marine Science, 11, 10.3389/fmars.2024.1277595, 2024.

Moriyasu, R., Evans, N., Bolster, K. M., Hardisty, D. S., and Moffett, J. W.: The Distribution and Redox Speciation of Iodine in the Eastern Tropical North Pacific Ocean, Global Biogeochemical Cycles, 34, e2019GB006302, https://doi.org/10.1029/2019GB006302, 2020.

Moriyasu, R., Bolster, K. M., Hardisty, D. S., Kadko, D. C., Stephens, M. P., and Moffett, J. W.: Meridional Survey of the Central Pacific Reveals Iodide Accumulation in Equatorial Surface Waters and Benthic Sources in the Abyssal Plain, Global Biogeochemical Cycles, 37, e2021GB007300, https://doi.org/10.1029/2021GB007300, 2023.

Qi, Y., Matsuzaki, H., Yamagata, T., and Nagai, H.: Iodine cycling in the subarctic Pacific Ocean: Insights from 129I, Geochim. Cosmochim. Acta, 344, 12-23, https://doi.org/10.1016/j.gca.2023.01.006, 2023.

Rapp, I., Schlosser, C., Browning, T. J., Wolf, F., Le Moigne, F. A. C., Gledhill, M., and Achterberg, E. P.: El Niño-Driven Oxygenation Impacts Peruvian Shelf Iron Supply to the South Pacific Ocean, Geophys. Res. Lett., 47, e2019GL086631, https://doi.org/10.1029/2019GL086631, 2020.

Schnur, A. A., Sutherland, K. M., Hansel, C. M., and Hardisty, D. S.: Rates and pathways of iodine speciation transformations at the Bermuda Atlantic Time Series, Frontiers in Marine Science, 10, 10.3389/fmars.2023.1272870, 2024.

Ştreangă, I.-M., Repeta, D. J., Blusztajn, J. S., and Horner, T. J.: Speciation and cycling of iodine in the subtropical North Pacific Ocean, Frontiers in Marine Science, 10, 10.3389/fmars.2023.1272968, 2024.

Truesdale, V. W., Bale, A. J., and Woodward, E. M. S.: The meridional distribution of dissolved iodine in near-surface waters of the Atlantic Ocean, Progress in Oceanography, 45, 387-400, https://doi.org/10.1016/S0079-6611(00)00009-4, 2000.

Waite, T. J., Truesdale, V. W., and Olafsson, J.: The distribution of dissolved inorganic iodine in the seas around Iceland, Mar. Chem., 101, 54-67, https://doi.org/10.1016/j.marchem.2006.01.003, 2006.

Xing, S., Hou, X., Shi, K., Aldahan, A., and Possnert, G.: Circulation of Circumpolar Deep Water and marine environment traced by ^{127}I and ^{129}I speciation in the Amundsen Sea Polynya, Antarctica, J. Environ. Radioact., 225, 106424, https://doi.org/10.1016/j.jenvrad.2020.106424, 2020.

Yang, M., Phillips, D. P., Hopkins, F. E., Liss, P., Suntharalingam, P., Carpenter, L. J., Chance, R., Brown, L. V., Stapleton, C. G., Jones, M. R., and Dall'Olmo, G.: Marine Biogeochemical Control on Ozone Deposition Over the Ocean, Geophys. Res. Lett., 52, e2024GL113187, https://doi.org/10.1029/2024GL113187, 2025.

Zhang, L., Hou, X., Gwynn, J. P., Karcher, M., Chen, N., Fan, Y., and Liu, Q.: Spatial variation and species transformation of 129I and 127I in the Central Arctic Ocean, Earth and Planetary Science Letters, 612, 118165, https://doi.org/10.1016/j.epsl.2023.118165, 2023.